

THREE-DIMENSIONAL FEATURES OF COHERENT FINE SCALE EDDIES IN TURBULENCE

Mamoru Tanahashi, Shiki Iwase, Md. Ashraf Uddin and Toshio Miyauchi
Department of Mechano-Aerospace Engineering, Tokyo Institute of Technology
Ookayama, Meguro-ku, Tokyo 152-8552, Japan

ABSTRACT

Three-dimensional structure of coherent fine scale eddies in turbulence is investigated by using a DNS database of a homogeneous isotropic turbulence. The axes of coherent fine scale eddies are determined and characteristics are clarified. The axis has several nodes which are identified as the minima of second invariant on the axis. Along the axis, maximum azimuthal velocity and axial velocity show relatively large fluctuations, while diameter is nearly constant. At each node, the axis bends with a large angle. Magnitude of advection velocity and direction of movement of the coherent fine scale eddy also change at these nodes. Probability density function of length of the segment between neighboring nodes shows a peak at the length of Taylor micro scale. The segment length shows a strong correlation with the maximum second invariant and increases with the increase of the second invariant with a $1/2$ - $2/3$ power. Probability density function of advection velocity of each segment of the axis shows a peak at 1.25 times of r. m. s. velocity fluctuation, which means that coherent fine scale eddies are very active in turbulence.

INTRODUCTION

The fine scale structure of turbulence is one of the most important subjects in turbulence researches, because the lack of the knowledge about the fine scale motions prevents developments of the proper turbulence theory and turbulent models. In the theories of small scale structure, many tube-like and sheet-like vortices have been considered as smallest structures in turbulence (Townsend, 1951; Tennekes, 1968; Lundgren, 1982; Pullin *et al.*, 1993). Recent direct

numerical simulations of homogeneous turbulence (She *et al.*, 1990; Vincent and Meneguzzi, 1991; Jimenez *et al.*, 1993) have shown that fine scale tube-like structures are present in homogeneous turbulence. In our previous studies (Tanahashi *et al.*, 1996; 1997a; 1997b; 1999a), we have identified the cross-sections on axes of coherent tube-like eddies from DNS data of homogeneous isotropic turbulence and have shown that mean diameter of those eddies is about 10 times of Kolmogorov micro scale (η) and the maximum of mean azimuthal velocity is about a half of root mean square of velocity fluctuation (u_{rms}). The investigated cross-sections were selected to include local maximum of second invariant of the velocity gradient tensor on the axis of coherent tube-like eddies. The dependence of the structure of coherent fine scale eddies on Reynolds number is very weak. Tanahashi *et al.* (1997c, 1998) have applied same analyses to turbulent mixing layer and showed that tube-like eddies in fully-developed turbulent mixing layers are very similar to those in homogeneous isotropic turbulence. The vortical structures in turbulent channel flows also show characteristics similar to tube-like eddies in homogeneous isotropic turbulence (Tanahashi *et al.*, 1999b). These results suggest that turbulence have a universal fine scale structure which can be called as 'coherent fine scale structure' in turbulence. The distributions of coherent fine scale eddies are closely related with the anisotropic behavior of turbulent free-shear layers (Tanahashi *et al.*, 1998) and near-wall turbulence (Tanahashi *et al.*, 1999b). Since turbulent energy is highly dissipated around the coherent fine scale eddies, the coherent fine scale structure plays an important role in the dissipation of total turbulent energy and its intermittent char-

acter (Tanahashi *et al.*, 1999a).

To understand the details of fine scale motions of turbulence, investigations of three-dimensional features of the coherent fine scale eddies are required. In this study, axes of coherent fine scale eddies are identified in homogeneous isotropic turbulence. Detail structure of several coherent fine scale eddies is presented and then statistical properties related to the three-dimensional structure are discussed.

IDENTIFICATION OF AXES OF COHERENT FINE SCALE EDDIES

DNS Data Base

In this study, DNS data of decaying homogeneous isotropic turbulence which have conducted by Tanahashi *et al.* (1997a, 1997b) are analyzed. Reynolds number based on u_{rms} and Taylor micro scale of the DNS data is $Re_\lambda=37.1$.

Identification scheme

Figure 1 shows contour surfaces of second invariant of velocity gradient tensor for $Re_\lambda=37.1$. The second invariant is defined as follows:

$$Q = \frac{1}{2}(W_{ij}W_{ij} - S_{ij}S_{ij}), \quad (1)$$

where S_{ij} and W_{ij} denotes symmetric and asymmetric part of the velocity gradient tensor, respectively. The visualized region is 1/8 of whole domain which is calculated by using 256^3 grid points. Length of the box in Fig. 1 is $2.84l$, 14.7λ or 165η , where l , λ and η are the integral length scale, Taylor micro scale and Kolmogorov micro scale, respectively. The second invariant is normalized by η and u_{rms} in Fig. 1 and the level of iso-surfaces is selected to be $Q^*=0.03$. Hereafter * denotes a variable normalized by η and u_{rms} . Figure 1 suggests that many tube-like structures exist in homogeneous isotropic turbulence. As discussed in Tanahashi *et al.* (1997a, 1999a), visualized regimes such as Fig. 1 depend significantly on the threshold of variables. The identification scheme which is independent on the threshold should be developed to investigate the essential aspects of fine scale structure of turbulence.

In the previous studies (Tanahashi *et al.*, 1997b: 1999a), we have identified the cross-sections of coherent fine scale eddies in homogeneous isotropic turbulence. The definition of eddy is 'rotating motion of fluid element around a certain point'. The identification scheme consists of the following steps:

- Evaluation of Q at each collocation point from the results of DNS.
- Probability of existence of positive local maximum of Q near the collocation points is evaluated at each collocation point from Q distribution. Because the case that a local maximum of Q coincides with a collocation point is very rare, it is necessary to define

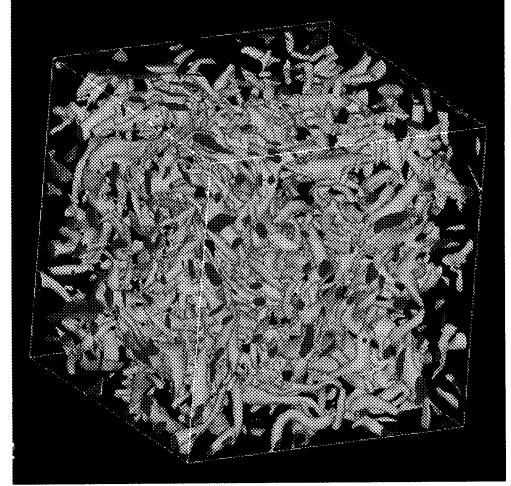


Figure 1. Contour surfaces of the second invariant of the velocity gradient tensor ($Q^*=0.03$).

probability on collocation points.

- Collocation points with non-zero probability are selected to survey actual maxima of Q . Locations of maximal Q are determined within the accuracy of 10^{-6} in terms of relative error of Q by applying a three dimensional cubic Spline interpolation to DNS data.
- A cylindrical coordinate system (r, θ, z) is considered by setting the maximal point as the origin. The coordinate system is assumed to have advection velocity at the origin. The z direction is selected to be parallel to the vorticity vector at the maximal point. The velocity vectors are projected on this coordinate and azimuthal velocity u_θ is calculated.
- Point that has small variance in azimuthal velocity compared with surroundings is determined. If the azimuthal velocities at $r = 1/5$ computational grid space show same sign for all θ , that point is identified as the center of the swirling motion.
- Statistical properties are calculated around the point. From the center of the cross-section (x_s), axes of each coherent fine scale eddies are searched by using a following auto-tracing algorithm which has reported by Tanahashi *et al.* (1997a).
- From x_s , the investigated point is moved in the axial direction with short distance ds . ds is parallel to the vorticity vector at x_s . A new cylindrical coordinate system (r', θ', z') is considered by setting the new point as the origin. On the (r', θ') plane with $z'=0$, the point with maximum Q is determined, and the steps (c) – (e) are applied.
- Central axis is determined by repeating the step (g). In this procedure, $|ds|$ is set equal to $1/5$ computational grid space. If angle (ϕ_n) between x_{n-1} and x_n is greater than 30 degree, the step (g) is applied again with $|ds'| = |ds| \cos(\phi_n)$.

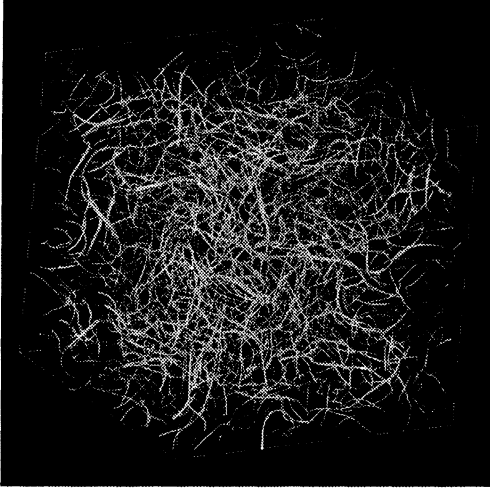


Figure 2. Axes of coherent fine scale eddies in a decaying homogeneous isotropic turbulence.

- (i) After the calculation of statistical properties, above steps are repeated until second invariant on the axis becomes negative or swirling motion can not be detected.
- (j) The steps (g) – (i) are conducted in the opposite direction of vorticity vector at \mathbf{x}_s .
- (k) The steps (g) – (j) are applied for the next starting point.

This identification scheme is applied for DNS data of decaying homogeneous isotropic turbulence. Figure 2 shows the distribution of axes of the coherent fine scale eddies for $Re_\lambda=37.1$. The visualized regime is the same in Fig. 1. Visualized diameters of the axes are drawn to be proportional to the square root of the second invariant on the axis. Larger diameter corresponds to stronger swirling motion. The comparison of Figs. 1 and 2 shows that the identified axes coincide with tube-like structures which are visualized by contour surfaces of Q . As the identification scheme does not depend upon the strength of the fine scale eddy, Fig. 2 includes weak fine scale eddies, which are not visualized in Fig. 1.

THREE-DIMENSIONAL FEATURES OF COHERENT FINE SCALE EDDIES

Structure of a typical coherent fine scale eddy

Figure 3 shows an axis of typical coherent fine scale eddy for $Re_\lambda=37.1$. Visualized diameters are selected to be proportional to the square root of Q on the axis similar to Fig. 2. The axis in Fig. 3 has several sharp bends that are identified with the minima of second invariant on the axis. The parts between bends seem to show relatively large second invariant and to be nearly straight. Figure 4 shows distributions of second invariant and third invariant on the



Figure 3. Axis of a typical coherent fine scale eddy.

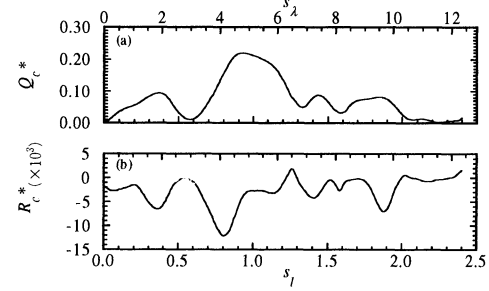


Figure 4. Second and third invariant on the axis of the typical coherent fine scale eddy. (a): second invariant, (b): third invariant.

typical coherent fine scale eddy. Here, s represents the coordinate along the axis. s_l and s_λ is normalized by l and λ respectively and the origin of s is shown in Fig. 3 by an arrow. The length of this eddy is about $2.4l$, 12.3λ or 150η . The identification procedures are stopped because second invariant on the axis becomes negative at the end of s_l (s_λ) = 0 and distinct swirling motion can not be observed at the other end. The second invariant shows relatively large fluctuation on the axis, and several minima of Q exist. In this study, we define the point on the axis with the minima of Q as a node of the coherent fine scale eddy. The coherent fine scale eddy in Fig. 3 has 5 nodes. The sign of the third invariant represents the local stretching and compression of the fluid element (Chong *et al.*, 1990). Figure 4(b) shows that most parts of the axis show negative third invariant, and that this eddy is continuously stretched along the axis. The third invariant seems to increase at the nodes where second invariant decrease, which means that the stretching rate on the axis decreases at the nodes.

Figure 5 shows maximum value of mean azimuthal velocity on the cross section, axial velocity on the axis and diameter for the typical eddy. In this study, radius of the eddy is defined by a distance between the center and location where the mean azimuthal velocity reaches to the maximum value. As shown in our previous studies (Tanahashi *et al.* 1997c: 1999a), azimuthal velocity of the coherent fine scale eddy is of the order of u_{rms} . Fluctuation of maximum azimuthal velocity along the axis is well correlated with that of second invariant (Fig. 4(a)). The sections with large second invariant show large azimuthal velocities. The axial velocity component is zero at $s_l = 1.4$

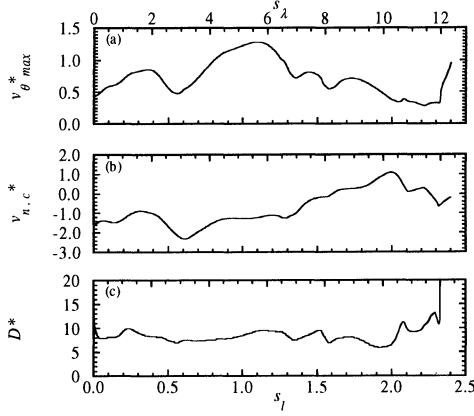


Figure 5. Distributions of maximum azimuthal velocity (a), axial velocity (b) and diameter (c) of the typical coherent fine scale eddy along the axis.

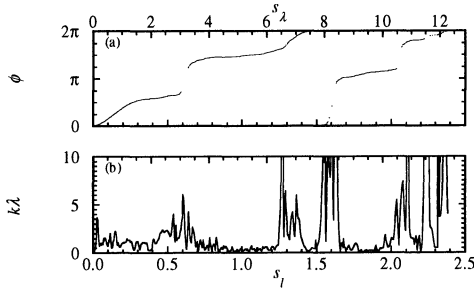


Figure 6. Inclination of axis of the typical coherent fine scale eddy (a) and curvature of the axis (b).

and increases along the axis with relatively weak fluctuations. The magnitude of the axial velocity component is relatively large and is of the order of u_{rms} . Contrary to the large fluctuation of maximum azimuthal velocity in Fig. 5(a), diameters of the coherent fine scale eddy are nearly constant along the axis and about 8η . Therefore, the fluctuation of magnitude of swirling motion, which is represented by the second invariant on the axis in Fig. 4(a), is caused by the azimuthal velocity.

As shown in Fig. 3, the central axis of the coherent fine scale eddy bends with large angle at the nodes. Figure 6 shows inclination angle (ϕ) and curvature (k) of the typical axis. The inclination angle is integrated from the origin and the curvature is normalized by Taylor micro scale. The segments between nodes are nearly straight, while the axis bends with large angles at the nodes. At each node, the axis turns the nose with about π . The curvature of the parts with relatively large second invariant is nearly constant and the radius of the curvature is larger than Taylor micro scale. At the nodes, however, the curvature is quite large.

As shown in the above, the coherent fine scale eddies show strong swirling motion around the axis and have distinct three-dimensional character. These eddies are moving

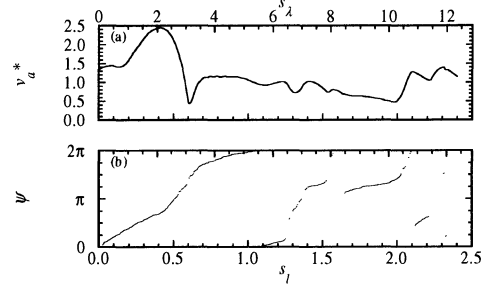


Figure 7. Magnitude of advection velocity in the radial direction (a) and direction of the advection velocity in r - θ plane (b).

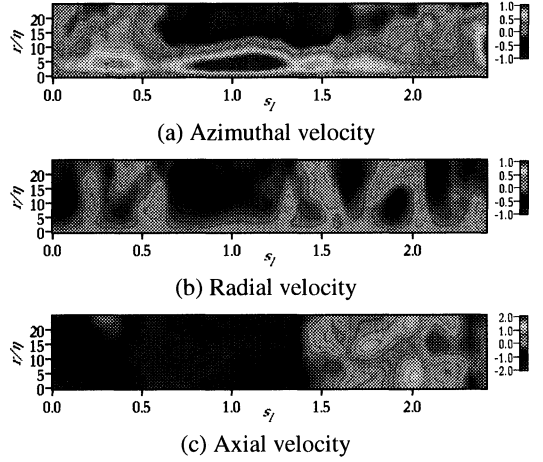


Figure 8. Mean velocity distributions along the typical coherent fine scale eddy.

in turbulence field with large advection velocity (Tanahashi *et al.* 1999a). The advection velocities in the radial direction on each section are shown in Fig. 7(a). The total advection velocity of the fluid elements near the central axis is represented by a sum of axial velocity in Fig. 5(b) and the radial advection velocity in Fig. 7(a). Although we discussed only the radial advection velocity because the axial velocity on the axis does not correspond to the advection of the eddy if the coherent fine scale eddy can be locally approximated by a stretched Burgers' vortex. In the case of the stretched Burgers' vortex, axial velocity is induced by the outer strain field, while the vortex has no advection velocity. Figure 7(a) suggests that the advection velocity in the radial direction is also order of u_{rms} and fluctuation of that is relatively small in the segments between the nodes. Figure 7(b) shows the direction of the advection in a (r, θ) plane. The coherent fine scale eddy changes its direction of advection drastically at every node. These angles are order of π similar to the inclination angle in Fig. 6(a). In other parts, the direction changes very slowly. These results imply that segments of the coherent fine scale

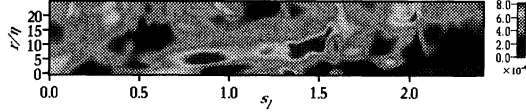


Figure 9. Mean dissipation rate distribution along the typical coherent fine scale eddy.

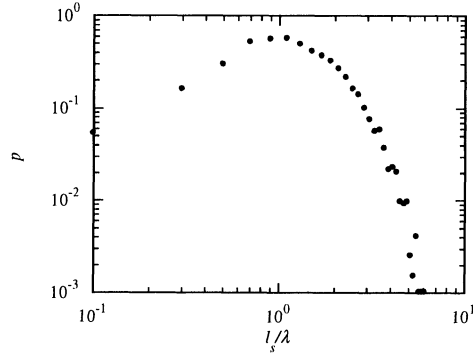


Figure 10. Probability density function of the segment length of coherent fine scale eddies.

eddies which are divided by the nodes are moving in other directions respectively.

Figure 8 shows the distributions of mean velocity around the typical axis. As described in the above, the distribution of mean azimuthal velocity shows the existence of distinct swirling motion around the axis. Furthermore, there are radial flows to the center from the ambient. The incoming flows are nearly uniform in the segments between the nodes. The strong axial flow can be observed not only on the axis but also in the regimes far from the central axis.

Figure 9 shows distribution of mean energy dissipation along the axis. The coherent fine scale eddies has important roles in the dissipation of turbulent energy and intermittent character of that (Tanahashi *et al.*, 1999a). Around the typical axis discussed in this section, maxima of azimuthal-averaged energy dissipation rate reaches to twice of volume-averaged value.

The same analyses were applied for several coherent fine scale eddies in homogeneous isotropic turbulence. The results obtained for other eddies were quite similar to the above, while total length of coherent fine scale eddies seems to depend upon the maximum second invariant on the axis.

Statistics of coherent fine scale eddies in homogeneous isotropic turbulence

In the previous section, it is shown that the characteristics of the central axes are drastically changed at the nodes where second invariant on the axis has minima. In this section, statistical properties concerning to the segments between the nodes are presented.

Figure 10 shows the probability density function (pdf) of

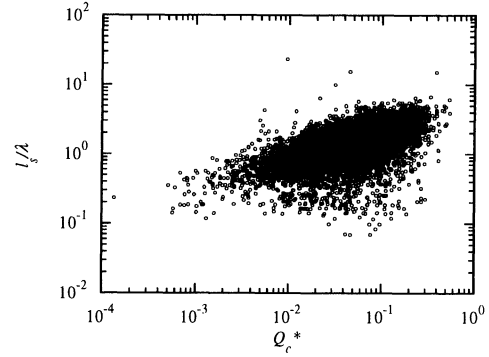


Figure 11. Relations between segment length and maximum second invariant in the segment.

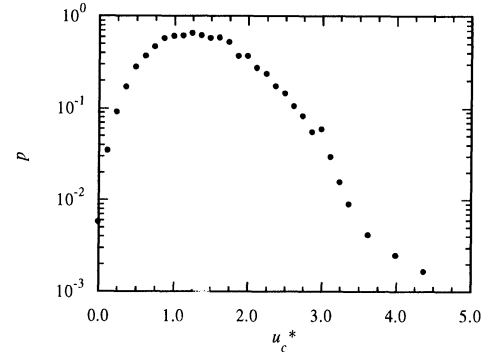


Figure 12. Probability density function of the advection velocity of the segments of coherent fine scale eddies.

the segment length of coherent fine scale eddies. The segment length is normalized by Taylor micro scale. The pdf of the segment length shows a peak at Taylor micro scale. The general physical interpretation of Taylor micro scale is that Taylor micro scale represents the mean size of fine scale eddies in turbulence, while this definition is quite obscure. Our result in Fig. 10 implies that coherent fine scale structure is directly related with Taylor micro scale. The coherent fine scale eddies educed in present studies have several nodes and total length is of the order of integral length scale. Therefore, the coherent fine scale structure includes three important length scale of turbulence: η , λ and l . It should be noted that diameter of coherent fine scale eddies can be scaled by Kolmogorov micro scale (Tanahashi *et al.*, 1997b: 1999a).

The relations between segment length and maximum second invariant in the segment are plotted in Fig. 11. The length of each segment shows strong correlation with the maximum second invariant in the segment. The segments with strong swirling motions that are denoted by large second invariant tend to be long. The segment length increases with the second invariant by a $1/2$ - $1/3$ power.

Figure 12 shows pdf of radial advection velocity where the second invariant on the axis becomes maximum value in

each segment of coherent fine scale eddy. The radial advection velocities are normalized by u_{rms} . As shown in Fig. 7, the advection velocity in the radial direction and its direction scarcely changes in the segment. Therefore, the radial advection velocity of the segment can be approximated by that at the center point with maximum second invariant in the segment. The pdf in Fig. 12 shows a peak at $1.25u_{rms}$. The largest advection velocity is over $4u_{rms}$. The pdfs of velocity fluctuation in homogeneous isotropic turbulence shows Gaussian distribution and the maximum value is about $4 - 5u_{rms}$ for this Reynolds number. This result shows that the motion of the axes of the coherent fine scale eddies is very active in turbulence.

CONCLUSIONS

In this study, three-dimensional features of coherent fine scale eddies in homogeneous isotropic turbulence are investigated. Following conclusions are obtained from our study.

- (1) The axes of the coherent fine scale eddy have several nodes which are identified as the minima of second invariant of the velocity gradient tensor on the axis. Along the axis, maximum azimuthal velocity and axial velocity show relatively large fluctuations, while diameter is nearly constant.
- (2) At each node, the axis bends with a large angle. Magnitude of advection velocity and direction of movement of the coherent fine scale eddy also change at these nodes.
- (3) Probability density function of length of the segment between neighboring nodes shows a peak at the length of Taylor micro scale. The segment length shows a strong correlation with the maximum second invariant and increases with the increase of the second invariant with a $1/2-2/3$ power.
- (4) Probability density function of advection velocity of each segment of the axis shows a peak at 1.25 times of r. m. s. velocity fluctuation, which means that coherent fine scale eddies are very active in turbulence.

ACKNOWLEDGEMENT

This work is partially supported by Grant-in-Aid for Scientific Research of the Ministry of Education, Science, Sports and Culture (No. 09450088).

REFERENCE

Chong, M. S., Perry, A. E. and Cantwell, B. J., 1990, "A General Classification of Three-Dimensional Flow Field," *Phys. Fluids*, Vol. A2, pp. 765-777.

Lundgren, T. S., 1982, "Strained Spiral Vortex Model for Turbulent Fine Structure", *Phys. Fluids*, Vol. 25, pp.2193-2203.

Pullin, D. I. and Saffman, P. G., 1993, "On the Lundgren-Townsend Model of Turbulent Fine Scales", *Phys. Fluids*, Vol. A5, pp. 126-145.

She, Z. -S., Jackson, E. and Orszag, S. A., 1990, "Intermittent Vortex Structures in Homogeneous Isotropic Turbulence", *Nature*, Vol. 344, pp. 226-228

Jimenez, J., Wray, A. A., Saffman, P. G. and Rogallo, R. S., 1993, "The Structure of Intense Vorticity in Isotropic Turbulence", *J. Fluid Mech.*, Vol. 255, pp. 65-90.

Jimenez, J. and Wray, A. A., 1998, "On the Characteristics of Vortex Filaments in Isotropic Turbulence", *J. Fluid Mech.*, Vol. 373, pp. 255-285.

Tanahashi, M., Miyauchi, T. and Yoshida, T., 1996, "Characteristics of Small Scale Vortices related to Turbulent Energy Dissipation", *Transport Phenomena in Thermal-Fluid Engineering.*, Vol. 2, pp. 1256-1261.

Tanahashi M., Miyauchi, T. and Ikeda, J., 1997a, "Identification of Coherent Fine Scale Structure in Turbulence", *Proceedings of IUTAM Symposium: Simulation and Identification of Coherent Structure in Flow*, in press.

Tanahashi, M., Miyauchi, T. and Ikeda, J., 1997b, "Scaling Law of Coherent Fine Scale Structure in Homogeneous Isotropic Turbulence", *Proceedings 11th Symposium on Turbulent Shear Flows*, Vol. 1, pp. 4-17.

Tanahashi, M., Miyauchi, T. and Matsuoka, K., 1997c, "Coherent Fine Scale Structure in Temporally-Developing Turbulent Mixing Layer", *Turbulence, Heat and Mass Transfer*, Vol. 2, p. 461, Delft University Press.

Tanahashi, M., Miyauchi, T., and Matsuoka, K., 1998, "Statistics of Coherent Fine Scale Structure in Turbulent Mixing Layers", to be appeared in *Proceedings of IUTAM/IUGG Symposium on Developments in Geophysical Turbulence*.

Tanahashi, M., Iwase, S., Ikeda, J. and Miyauchi, T., 1999a, "Coherent Fine Scale Structure in Homogeneous Isotropic Turbulence", preparing

Tanahashi, M., Das, S. K., Shoji, K. and Miyauchi, T., 1999b, "Coherent Fine Scale Structure in Turbulent Channel Flows", submitted to *Trans. JSME*.

Tennekes, H., 1968, "Simple Model for the Small-Scale Structure of Turbulence", *Phys. Fluids*, Vol. 11, pp. 669-761.

Townsend, A. A., 1951, "On the Fine-Scale Structure of Turbulence", *Proc. R. Soc. Lond.*, Vol. A208, pp. 534-542.

Vincent, A. and Meneguzzi, M., 1991, "The Spatial Structure and Statistical Properties of Homogeneous Turbulence", *J. Fluid Mech.*, Vol. 225, pp. 1-20.